CHEMICAL ENGINEERING TRANSACTIONS
VOL. 61, 2017
A publication of AIDIC
The Italian Association of Chemical Engineering
Online at www.aidic.it/cet
Guest Editors: Petar S Varbanov, Rongxin Su, Hon Loong Lam, Xia Liu, Jiří J Klemeš

ISBN 978-88-95608-51-8; **ISSN** 2283-9216
DOI: 10.3303/CET1761295

Simulation and Optimization of a Continuous Reverse Osmosis Desalination Process for Making Fresh Water

Fatemehsadat Mirghaderi[a], Nejat Rahmanian[a,*], Raj Patel[a], Davide Manca[b], Iqbal M. Mujtaba[a]

[a]Chemical Engineering Division, School of Engineering, University of Bradford, BD7 1DP, UK
[b]PSE-Lab-Dipartimento di Chimica, Materiali e Ingegneria Chimica "G. Natta", Politecnico di Milano, Piazza Leonardo da Vinci 32, 20133 Milan, Italy
n.rahmanian@bradford.ac.uk

Despite being a mature process, production of fresh water using desalination is still a challenge. Desalination is broadly divided into two categories; thermal desalination processes, such as multi-stage flash, and semi-permeable membrane process, such as Reverse Osmosis (RO). This work is aimed at developing correlations for water permeability coefficient (K_w) and salt permeability coefficient (K_s) as a function of feed salinity and pressure using experimental data for a continuous RO process. For three different feed salinities of 15, 25, and 35 g/L at two different pressures of 40 and 45 bara experimental values of K_s and k_w values are taken from the literature. Planar and ellipsoidal least square methods are used to correlate k_w and K_s as a function of feed salinity and pressure, which are then embedded within the continuous RO process model to evaluate the process performance in terms of maximising the recovery ratio while optimizing the area and pressure to get the desired freshwater salinity. gPROMS model builder is used to simulate and optimise the process.

1. Introduction

Desalination processes have emerged as the new sources of production of fresh water over the past few decades in terms of both operation (Barello, et al., 2015) and design (Patroklou et al., 2013). In the RO process, a semi-permeable membrane is used to separate salt and impurities from saline water (Charcosset, 2009). Desalination processes represent 53% of the desalination capacity globally (Mezher et al., 20110). The RO desalination process is characterised by high salt rejection (99.8 % for seawater desalination and 99 % for brackish water desalination) and high recovery ratio (Altaee, 2012).
Barello et al. (2015) studied batch the RO desalination process experimentally for several initial feed salinities of 15, 25, and 35 g/L at two different pressures of 40 and 45 bara and K_w and K_s correlations were developed as a function of salinity (which was continuously changing due to the batch process shown in Figure 1) and pressure. However, their correlations were not useful for continuous RO process (Figure 2) because the correlations were not only a function of initial feed salinity but also a function of changing salinity. To the best knowledge of the authors, this is the first work to develop correlations for the prediction of k_w and k_s as a function of feed salinity and pressure for a continuous process and where the correlations are embedded in the full process model in gPROMS to evaluate the performance of the process.

2. Continuous RO process model

Figure 2 shows a schematic diagram of a continuous reverse osmosis desalination plant, where the feed salinity and feed flow are constant. The process model is taken from (El-Dessouky and Ettouney, 2002) and more recent work of Barello et al. (2015).

$$Kw = \frac{M_p}{(\Delta P - \Delta\pi)AC_1} \quad (1)$$

Please cite this article as: Mirghaderi F., Rahmanian N., Patel R., Manca D., Mujtaba I.M., 2017, Simulation and optimization of a continuous reverse osmosis desalination process for making fresh water, Chemical Engineering Transactions, 61, 1783-1788 DOI:10.3303/CET1761295

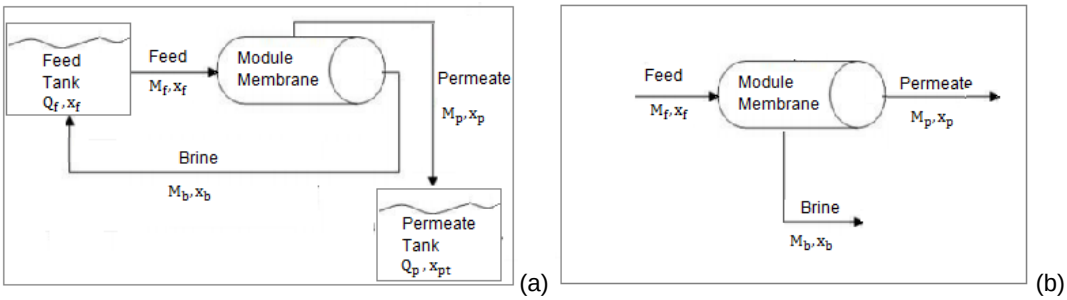

Figure 1: (a) Batch RO process (Barello et al., 2015); (b) Schematic diagram of a continuous RO process

$$\bar{\pi} = 0.5(\pi_f + \pi_b) \quad (2)$$

$$\Delta\pi = \bar{\pi} - \pi_p \quad (3)$$

where, $M_p(L/min)$, A (m2),$\bar{\pi}$ (bara), $\Delta\pi$ (bara) and ΔP(bara) are permeate flow, area, average osmotic pressure on the feed side, net osmotic pressure differential across the membrane, and the pressure difference between the feed and permeate sides of the membrane. The osmotic pressures can be calculated by using the following equations:

$$\pi_b = 0.7573 * x_b \quad (4)$$

$$\pi_f = 0.7573 * x_f \quad (5)$$

$$\pi_p = 0.7573 * x_p \quad (6)$$

where, π_b, π_f and π_p are brine, feed and permeate osmotic pressure in bara, x_b, x_f and x_p are brine, feed and permeate salinity in g/l, respectively.

$$M_b = M_f - M_p \quad (7)$$

$$Ks = \frac{J_s}{(\bar{x} - x_p)} \quad (8)$$

where J_s is the rate of salt transport through the membrane. The average salinity, $\bar{x}$ can be found as:

$$\bar{x} = \frac{M_f x_f - M_b x_b}{M_f + M_b} \quad (9)$$

$$x_p = \frac{J_s}{M_p} \quad (10)$$

$$M_b x_b = M_f x_f - M_p x_p \quad (11)$$

The relationship between the length of the membranes and membrane area for the experimental study of Barello et al. (2015) is given by the following Eq(12):

$$L = 12.5 * A \quad (12)$$

Finally, the recovery ratio (RR) can be defined as:

$$RR = \frac{M_p}{M_f} * 100 \quad (13)$$

3. Methodology

In this work, the planar and ellipsoidal least square methods have been used to develop the Kw and k_s correlations. The aim of using the least square method is to minimize the difference between experimental data and predicted values from the process model.
Eq(14) (Eberly, 1999) shows the planar least square method:

$$z = ax + by + c \quad (14)$$

In Eq(14), it is possible to find the equation coefficients by solving a system of 3 equations and 3 unknowns. In doing so, one can form a 3 x 1 matrix of coefficients D, where D is: $D = [a, b, c]$

The error function can be defined as follows:

$$E(a,b,c) = \sum_{i=1}^{m} [(ax_i + by_i + c) - z_i]^2 \quad (15)$$

Where m is the number of data points. The first derivative of this function with respect to a, b and c should be zero to minimize the error.
Setting $\frac{\partial E}{\partial a} = 0, \frac{\partial E}{\partial b} = 0$ and $\frac{\partial E}{\partial c} = 0$ would result in the following equation:

$$(0,0,0) = \nabla E = 2 * \sum_{i=1}^{m} [(ax_i + by_i + c) - z_i](x_i, y_i, 1) \quad (16)$$

Defining, in this case, the 6 x 3 matrix of variables, Q_i:

$$Q_i = \begin{bmatrix} x_1 & x_2 & x_3 & x_4 & x_5 & x_6 \\ y_1 & y_2 & y_3 & y_4 & y_5 & y_6 \\ 1 & 1 & 1 & 1 & 1 & 1 \end{bmatrix}$$

Rearrangement of Eq(16) results in:

$$\left(\sum_{i=1}^{m} Q_i Q_i^T\right) D = \left(\sum_{i=1}^{m} z_i Q_i\right) \quad (17)$$

Which results in the following arrangement:

$$\begin{bmatrix} \sum_{i=1}^{m} x_i^2 & \sum_{i=1}^{m} x_i y_i & \sum_{i=1}^{m} x_i \\ \sum_{i=1}^{m} x_i y_i & \sum_{i=1}^{m} y_i^2 & \sum_{i=1}^{m} y_i \\ \sum_{i=1}^{m} x_i & \sum_{i=1}^{m} y_i & \sum_{i=1}^{m} 1 \end{bmatrix} \begin{bmatrix} a \\ b \\ c \end{bmatrix} = \begin{bmatrix} \sum_{i=1}^{m} z_i x_i \\ \sum_{i=1}^{m} z_i y_i \\ \sum_{i=1}^{m} z_i \end{bmatrix} \quad (18)$$

The result is a system of three equations and three variables to find the equation coefficients. The least square solution is as follows:

$$z_i = ax_i + by_i + c \quad (19)$$

Eq(20) (Chaudhuri, 2010) shows the ellipsoidal least square method:

$$\frac{x^2}{a'^2} + \frac{y^2}{b'^2} + \frac{z^2}{c'^2} = 1 \quad (20)$$

The error function can be defined as Eq(21)

$$(0,0,0) = E(a,b,c) = \sum_{i=1}^{m} \left[\left(1 - \frac{x^2}{a'^2} - \frac{y^2}{b'^2} - \frac{z^2}{c'^2}\right)\right]^2 \quad (21)$$

The first derivative of the error function with respect to each coefficient should be zero to get the minimum error which means $\frac{\partial E}{\partial a} = 0$, $\frac{\partial E}{\partial b} = 0$ and $\frac{\partial E}{\partial c} = 0$ $(a \neq 0, b \neq 0 \text{ and } c \neq 0)$ which are illustrated by Eq(22) to (24):

$$\frac{\sum_{i=1}^{m} x_i^4}{a'^2} + \frac{\sum_{i=1}^{m} x_i^2 y_i^2}{b'^2} + \frac{\sum_{i=1}^{m} x_i^2 z_i^2}{c'^2} = \sum_{i=1}^{m} x_i^2 \quad (22)$$

$$\frac{\sum_{i=1}^{m} x_i^2 y_i^2}{a'^2} + \frac{\sum_{i=1}^{m} y_i^4}{b'^2} + \frac{\sum_{i=1}^{m} y_i^2 z_i^2}{c'^2} = \sum_{i=1}^{m} y_i^2 \quad (23)$$

$$\frac{\sum_{i=1}^{m} x_i^2 z_i^2}{a'^2} + \frac{\sum_{i=1}^{m} y_i^2 z_i^2}{b'^2} + \frac{\sum_{i=1}^{m} z_i^4}{c'^2} = \sum_{i=1}^{m} z_i^2 \quad (24)$$

Replacing $\frac{1}{a'^2}$, $\frac{1}{b'^2}$ and $\frac{1}{c'^2}$ with a, b and c result in:

$$a\sum_{i=1}^{m} x_i^4 + b\sum_{i=1}^{m} x_i^2 y_i^2 + c\sum_{i=1}^{m} x_i^2 z_i^2 = \sum_{i=1}^{m} x_i^2 \quad (25)$$

$$a\sum_{i=1}^{m} x_i^2 y_i^2 + b\sum_{i=1}^{m} y_i^4 + c\sum_{i=1}^{m} y_i^2 z_i^2 = \sum_{i=1}^{m} y_i^2 \quad (26)$$

$$a\sum_{i=1}^{m} x_i^2 z_i^2 + b\sum_{i=1}^{m} y_i^2 z_i^2 + c\sum_{i=1}^{m} z_i^4 = \sum_{i=1}^{m} z_i^2 \quad (27)$$

By solving the system of three equations and three unknowns, one can obtain the equations coefficients.

4. Results and discussion

Table 1 shows the results for water permeability coefficient. According to Table 1, Eq(20) generally gives more accurate results than Eq(14). The coefficients of are given in Table 2. Figure 3 compares the simulation and experimental results for pressures of 40 and 45 bara under three different feed salinities of 15, 25, and 35 g/L from Eq(14) and Eq(20). These figures confirm the accuracy of the ellipsoidal least square method.
A similar procedure was conducted for salt permeability coefficient (K_s) and the results are shown in Table 3. The calculated errors from both Eq(14) and Eq(20) are listed in Table 3 indicating the best method. Similarly, the results from Eq(20) are highly accurate and close to the experimental data. Coefficients of Eq(14) and (20) for salt permeability coefficient are given in Table 4. Figure 4 shows the experimental and simulation results from Eq(14) and(20) for salt permeability coefficients.

Table 1: Experimental and simulation results for water permeability coefficients.

	x_{f0}(g/l)	ΔP(bara)	Kw(experiment)	Kw Eq(14)	Kw Eq(20)	Error Eq(14)	Error Eq(20)
1	15	40	2.41×10^{-5}	2.31×10^{-5}	2.45×10^{-5}	1.00×10^{-5}	4.00×10^{-7}
2	25	40	2.32×10^{-5}	2.14×10^{-5}	2.32×10^{-5}	1.70×10^{-5}	4.00×10^{-8}
3	35	40	2.11×10^{-5}	1.65×10^{-5}	2.09×10^{-5}	4.30×10^{-5}	2.00×10^{-7}
4	15	45	2.57×10^{-5}	2.63×10^{-5}	2.52×10^{-5}	6.00×10^{-7}	5.00×10^{-7}
5	25	45	2.36×10^{-5}	2.47×10^{-5}	2.38×10^{-5}	1.10×10^{-6}	2.00×10^{-7}
6	35	45	2.15×10^{-5}	2.30×10^{-5}	2.16×10^{-5}	1.70×10^{-6}	1.00×10^{-7}

error=|experiment-simulation|

Table 2: Coefficient value of Eq(14) and Eq(20) for Kw

Coefficient	a	b	c
Eq(14)	-1.537151×10^{-7}	6.366329×10^{-7}	-8.4111676×10^{-8}
Eq(20)	3.20×10^{-4}	-1.48×10^{-4}	$1.93\times10\times10^{9}$

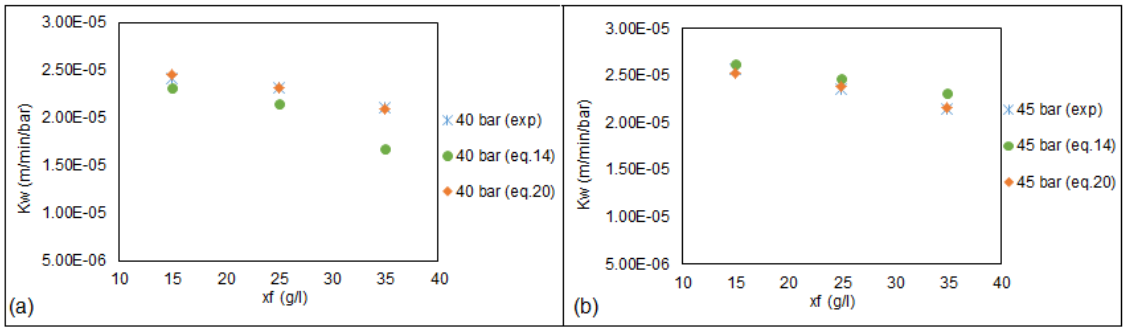

Figure 3: The simulation results for Kw at (a) 40 and (b) 45 bara pressure.

Table 3: Experimental and simulation results for salt permeability coefficient

	x_{f0}(g/l)	ΔP (bara)	Ks (experiment)	Ks Eq(14)	Ks E(20)	Error Eq(14)	Error Eq(20)
1	15	40	0.02172	0.020353	0.021847	1.37×10^{-3}	1.27×10^{-4}
2	25	40	0.0175	0.017616	0.019642	1.16×10^{-4}	2.14×10^{-3}
3	35	40	0.01517	0.011816	0.015767	3.35×10^{-3}	5.97×10^{-4}
4	15	45	0.02216	0.023415	0.022195	1.26×10^{-3}	3.52×10^{-5}
5	25	45	0.02117	0.020677	0.020029	4.93×10^{-4}	1.14×10^{-3}
6	35	45	0.01733	0.017939	0.016246	6.09×10^{-4}	1.08×10^{-3}

Experimental results obtained by Barello et al. (2015) showed that at constant pressure as the feed salinity increases, salt and water permeability coefficients decrease. The experimental results have also shown that at the constant feed salinity as the pressure increase, salt and water permeability coefficients will also increase.
In this work, the least square method was used to predict the Kw and Ks trends for higher and lower feed salinities and pressures. In doing so, three other operating pressure of 30, 50 and 60 bara and feed salinities in the range of 15 to 45 g/L were considered. As shown in Figure 5, the simulation results obtained by using Eq(20)

are in good consistency with the experimental data. Indeed, by increasing the feed salinity at constant pressure both Kw and Ks decrease. In addition, by increasing the pressure at constant feed salinity the water and salt permeability coefficients increase too.

Table 4: Coefficient values of Eq(14) and Eq(20) for Ks

Coefficient	a	b	c
Eq. 14	-2.74×10^{-4}	6.12×10^{-4}	-3.43×10^{-5}
Eq. 20	4.85×10^{-4}	-7.65×10^{-5}	2122.849

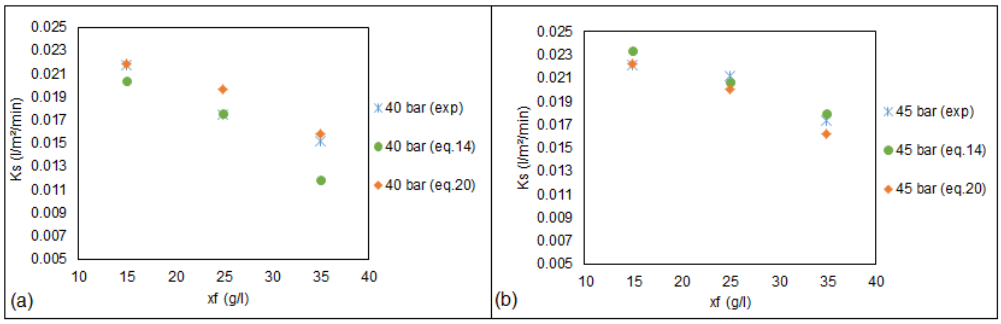

Figure 4: The simulation results for Ks at (a) 40 and (b) 45 bara pressure

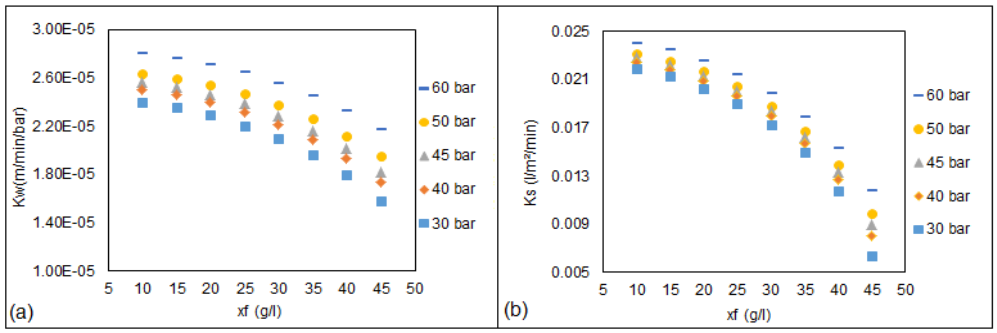

Figure 5: (a) Water salt permeability coefficient and (b) salt permeability coefficient prediction by using Eq(20)

According to WHO (World Health Organization, 2011) the total dissolved solids in drinking water should be well below 500 ppm. It is aimed to keep the total concentration of the impurities in the produced fresh water (permeate) in this simulation and optimization in the range of 200 - 205 ppm to guarantee the purity of the produced fresh water. Next, the model is used to maximize the recovery ratio by maintaining the permeate salinity in the range of 200 - 205 ppm and simultaneously optimizing pressure and area for a given feed flow and feed salinity. The feed flow-rate and feed salinity were considered to be $1000\ \mathrm{L/min}$ and $15\mathrm{L}$. Figure 2a shows the recovery ratio trend with respect to area and pressure.

$$\frac{x_f^2}{a'^2}+\frac{P^2}{b''^2}+\frac{k_w^2}{c'^2}=1 \tag{28}$$

$$\frac{x_f^2}{a'^2}+\frac{P^2}{b''^2}+\frac{k_s^2}{c'^2}=1 \tag{29}$$

In Eq(28), the feed salinity is considered constant. Coefficients of $\frac{1}{b'^2}$ and $\frac{1}{c'^2}$ are positive and negative, respectively. As the pressure increases the water permeability coefficient will also increase to keep the equality constraint. Similarly, in Eq(29), the coefficients of $\frac{1}{b'^2}$ and $\frac{1}{c'^2}$ are negative and positive. As the pressure rises, the salt permeability coefficient will increase to keep the equality constraint.

Eq(1) and (8) can be re-written as shown below. Eq(30) relates permeate flow to water permeability coefficient as well as area and pressure. Also, according to Eq(31), J_s is a function of salt permeability coefficient and pressure as well as $\bar{x}$ and area.

$$M_p = Kw * (\Delta P - \Delta\pi)AC_1 \quad (30)$$

$$J_s = Ks * (\bar{x} - x_p)A \quad (31)$$

According to Eq(30) and Eq(31), at a constant area as the pressure goes up, both Kw and $(\Delta P - \Delta\pi)$ would increase resulting in higher permeate flows. In addition, as the pressure goes up, Ks and J_s would increase. In this case, simulation results showed that the increment in M_p dominates the increment in J_s and results in lower permeate salinity, according to Eq(10).
After reaching a certain pressure, this trend would be opposite and as the pressure increases, the area would decrease to get the highest recovery ratio. By using gPROMS, it is possible to find the optimal area and pressure to get the highest possible permeate flow with the desired permeate salinity. Figure 6.b shows as the pressure increases recovery ratio increases.

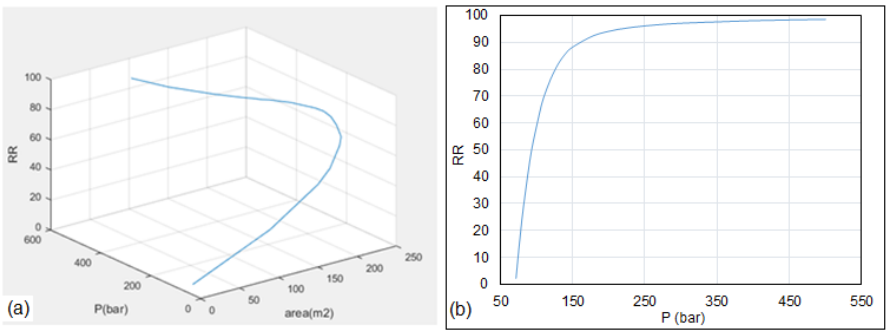

Figure 6: (a) Maximizing the RR with respect to area and pressure for the feed salinity of 15 g/L, (b) Recovery Ratio trend with respect to pressure for the feed salinity of 15 gL

5. Conclusions

The simulation and optimization of a continuous reverse osmosis desalination process was carried out by gPROMS. In doing so, two least square methods were used to predict the experimental results. The simulation results show that the ellipsoidal least square method is highly accurate and extrapolation and interpolation results obtained by this equation for water and salt permeability coefficients follow a similar trend to the experimental data. The simulation results for specific feed flow and feed salinity indicate the dependency of recovery ratio on required pressure and area for obtaining higher permeate flows and a desired permeate salinity.

References

Altaee A., 2012, Computational model for estimating reverse osmosis system design and performance: Part-one binary feed solution, Desalination, 291, 101-105.
Barello M., Manca D., Patel R., Mujtaba I.M., 2015, Operation and modeling of RO desalination process in batch mode, Computers and Chemical Engineering, 83, 139-156.
Charcosset C., 2009, A review of membrane processes and renewable energies for desalination, Desalination, 245, 214-231.
Chaudhuri D., 2010, A simple least squares method for fitting of ellipses and circles depends on border points of a two-tone image and their 3-D extensions, Pattern Recognition Letters, 31, 818–829.
Eberly D., 1999, Sample Applications: Mathematics, <www.geometrictools.com/> accessed 5.01.2015.
El-Dessouky H.T., Ettouney H.M., 2002, Fundamentals of Salt Water Desalinaiton, 1st Ed. Amsterdam, The Netherlands: Elsevier Science B.V.
Mezher T., Fath H., Abbas Z., Khaled A., 2011, Techno-economic assessment and environmental impacts of desalination technologies, Desalination, 266, 263-273.
Patroklou G., Sassi K.M., Mujtaba I.M., 2013, Simulation of boron rejection by seawater reverse osmosis desalination, Chemical Engineering Transactions, 32, 873-1878.
WHO, 2011, Guidelines for drinking-water quality, 4th ed. Surveillance and control of community supplies, <apps.who.int/iris/bitstream/10665/44584/1/9789241548151_eng.pdf> accessed 18.07.2017.